ACCESS

A SPACE CORONAGRAPH CONCEPT
FOR DIRECT IMAGING AND SPECTROSCOPY OF EXOPLANETARY SYSTEMS

John Trauger
Jet Propulsion Laboratory
California Institute of Technology
john.trauger@jpl.nasa.gov
818-354-9594

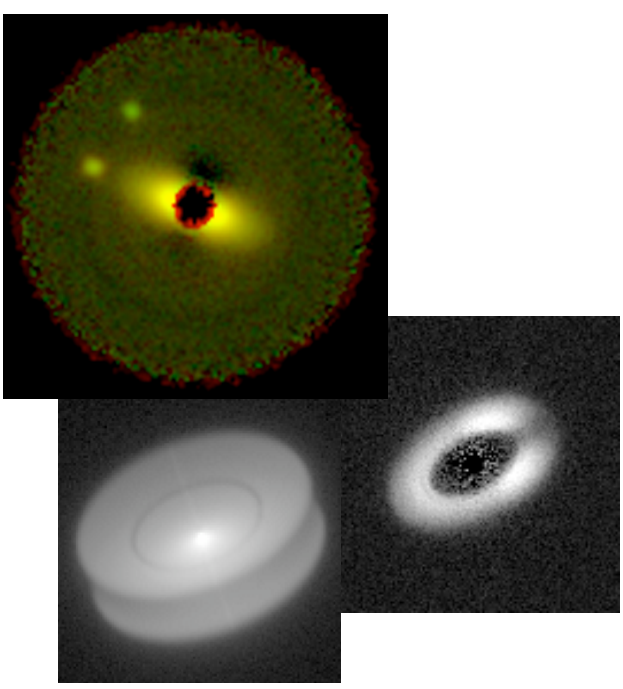

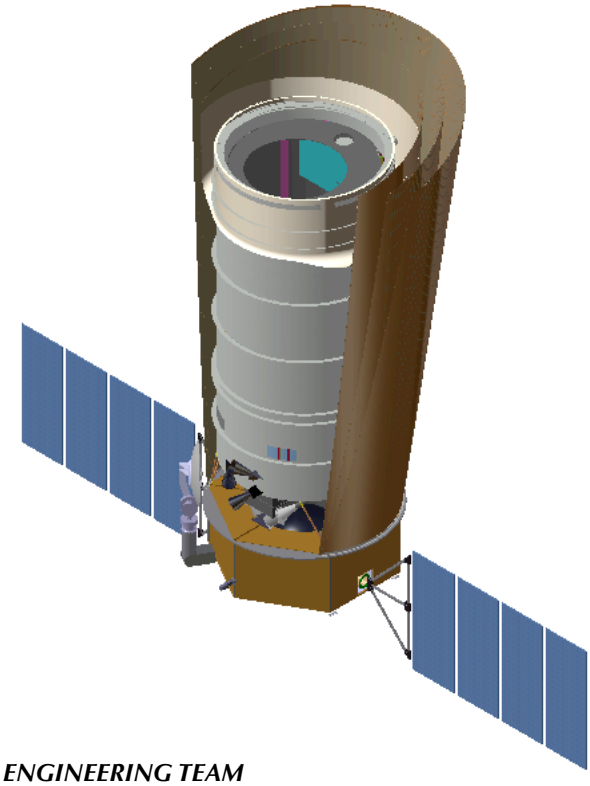

***ACCESS* SCIENCE AND ENGINEERING TEAM**

James Alexander, Paul Brugarolas, Olivia Dawson, Robert Gappinger, Curt Henry, John Krist, Dimitri Mawet, Virgil Mireles, Dwight Moody, Peggy Park, Laurent Pueyo, Eugene Serabyn, Stuart Shaklan, Karl Stapelfeldt, John Trauger, Wesley Traub (Jet Propulsion Laboratory, California Institute of Technology); Olivier Guyon (U. Arizona and Subaru Telescope); Ruslan Belikov (NASA/Ames); Jeremy Kasdin, David Spergel, Robert Vanderbei (Princeton University); Geoffrey Marcy (UC Berkeley); Robert A. Brown (STScI); Jean Schneider (Paris Observatory); Bruce Woodgate (NASA/Goddard); Gary Matthews, Robert Egerman, Phillip Vallone, Jason Elias, Perry Voyer, Yves Conturie (ITT Space Systems LLC); Ronald Polidan, Charles Lillie, Connie Spittler, David Lee, Reem Hejal, Allen Bronowick, Nick Saldivar (Northrop Grumman Aerospace Systems); Thomas Price, Mark Ealey (Northrop Grumman/Xinetics)

ACCESS

A SPACE CORONAGRAPH CONCEPT
FOR DIRECT IMAGING AND SPECTROSCOPY OF EXOPLANETARY SYSTEMS

Executive Summary

We outline the science potential and engineering readiness of a space mission for the direct coronagraphic imaging and spectroscopy of exoplanetary systems at visible wavelengths, the outcome of the ACCESS science and engineering investigation carried out as one of NASA's Astrophysics Strategic Mission Concept Studies. ACCESS has compared the four major coronagraph architectures (Lyot, vector vortex, pupil mapping, and shaped pupil) in the context of a conceptual space observatory platform of high technology maturity. The study has also compared recent physical demonstrations with JPL's High Contrast Imaging Testbed (HCIT) and other laboratories as a measure of technology readiness. We have selected one of these coronagraph types to represent the highest readiness level among the coronagraph architectures, for a reliable estimate of science performance available with today's technology and for a reliable determination of mission cost, risk, and schedule. We describe the exciting new science enabled by a NASA medium-class coronagraph mission that could be initiated in the coming year with proven high-maturity technologies.

The ACCESS telescope, spacecraft, and pointing systems are representative of the "best" available for exoplanet coronagraphy within the scope (cost, risk, schedule) of a NASA medium-class mission. ACCESS operates at visible wavelengths (500-900 nm) for high contrast imaging at small inner working angles, owing to the need to suppress diffracted light at small angular separations from the star. We note that all coronagraph types require an observatory system with exceptional pointing control, exceptional wavefront stability, and active wavefront control. ACCESS defines a baseline observatory architecture that fully supports any of the major coronagraph types, hence it is a platform that provides a meaningful performance comparisons among coronagraph types.

We believe that ACCESS is a capable and ready coronagraph mission for the study of exoplanetary systems, based on demonstrated technologies that are already at high levels of technology readiness. We outline further advancements in the area of coronagraph performance that could be achieved in the coming year, based on ongoing laboratory programs that are actively developing well-understood technologies.

ACCESS could make a nearly complete census of giant planets orbiting 3-20 AU from their parent stars and zodi dust structures at the level of our solar system, for over 100 nearby stars. A measure of the prevalence of exoplanetary systems, the first pioneering images and spectra of their exoplanets, observations of tell-tale asymmetries in the dust disks, all promise a wealth of new information, seeding further investigations of the nearby planetary systems, while laying the science and technology groundwork for still more ambitious programs of exoplanet exploration.

Science Case for a Medium Class Coronagraphic Imaging Mission

Planetary systems consist of gas giant planets, rocky terrestrial planets, and belts of small bodies which generate debris particles. Amazing progress has been made in their study over the past 14 years: More than 300 giant exoplanets have been detected indirectly by the radial velocity technique; more than 50 hot planets have been identified from transit observations, and thermal emission differentially measured from a small subset of them (Pont et al. 2009); infrared excesses indicative of debris disks as faint as 50× our Kuiper Belt have been detected in 15% of FGK stars (Trilling et al. 2008); and direct imaging has just revealed a few widely separated, very young planets orbiting their host stars (Kalas et al. 2008; Marois et al. 2008). These exciting discoveries, made with previously existing facilities (sometimes with modest instrument upgrades), offer a taste of the science returns that could be realized by a major new facility designed from the outset to meet the specific needs of exoplanet science.

Here we outline the science capabilities of ACCESS, a 1.5 meter space telescope and high-contrast coronagraph. We then review the current trajectory of exoplanet science with existing and developing astronomical facilities. Well beyond the advances anticipated on this trajectory, ACCESS offers the prospect of resolved images and spectra of planetary systems like our own, noting that to directly detect mature giant planets, exozodiacal dust structures at the levels found in our solar system, and terrestrial planets, nearby stars must to be probed at imaging contrasts of 10^{-9} or better. ACCESS is ready to carry out pioneering exoplanet science and general astrophysics as a medium-class NASA mission, while proving the technology and laying the scientific groundwork for still more ambitious future missions.

Exoplanet Science with ACCESS

Spectra of Known RV Planets Beyond 2 AU: Radial velocity (RV) surveys have singled out the nearby stars that host Jovian planets. Ten nearby stars are currently known to host RV planets whose apastron distances project to angular separations greater than the ACCESS inner working angle of 3 λ/D (0.23 arcseconds at λ= 550 nm). These are cold objects with a contrast of 10^{-9} in the optical and near-IR, and thus are only accessible to a space mission. Existing ephemerides allow observations to be timed to coincide with their maximum elongations, as indicated by the diagram at right. Thirteen additional stars within 20 pc show long-term accelerations indicating the presence of outer planets with orbits still not yet defined. ACCESS will directly detect these 23 giant planets, measure their colors, take spectra at R ~20, and provide astrometry that will resolve the *sin i* ambiguity in their masses. The spectra will allow the strength of CH_4 features to be measured and the depth of the uppermost cloud deck to be inferred. The planet's albedo and presence of bright ring systems can be inferred using the observed photometry and planet sizes estimated from their measured masses. Multi-epoch imaging showing the planetary orbital motions will make a powerful impression of the reality of exoplanetary systems in the public mind.

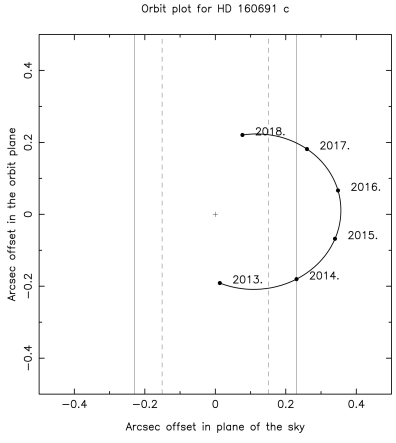

Planet Searches Beyond RV Survey Limits: RV searches to date have yielded detections of giant planets within 6 AU of (primarily) FGK stars with low chromospheric activity. Planets with longer periods or face-on orbits, and those orbiting active stars or A stars that lack a rich absorption spectrum, will escape RV detection. Two epochs of ACCESS imaging can detect objects to within

3 AU for stars within 15 pc, and in to 1 AU for perhaps a dozen targets. The stability of the ACCESS telescope will allow exoplanet detections down to contrasts of 10^{-10}, corresponding to a giant planet at 15 AU separation. Among the eighteen young stars (age < 1 Gyr) within 20 pc, ACCESS can detect any companions > 5 Jupiter masses in their thermal emission at z band. For searches of the 3-15 AU region, 3 epochs of observations spaced at the beginning, middle, and end of a five-year mission will provide a sufficient exploration of orbital phase space to achieve a detection completeness exceeding 70%. For the dozen stars where searches as close as 1 AU are possible, 6-10 epochs of imaging may be needed to compile good completeness results. The newly discovered planets will then be characterized spectroscopically. For a handful of the brightest and nearest stars, ACCESS performance may be good enough to detect terrestrial planets in the habitable zone (HZ), for low levels of exozodiacal dust.

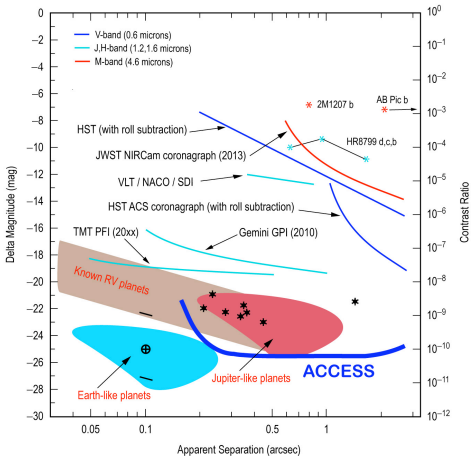

ACCESS exoplanet discovery space: ACCESS imaging sensitivity compared to other methods available now and in the coming decade. Shaded areas indicate the regions of high probability (from Monte-Carlo simulations) of detecting planets orbiting the nearest 100 AFGK stars. Jupiters in 5 AU orbits fall in the red-shaded area, where specific RV-identified planets are shown by asterisks. Earth-like planets fall in the blue-shaded area. The location of an Earth-twin at elongation at 10 pc is indicated by the ⊕ symbol, with a dash above for the background from a dust disk similar to the solar system, and a dash below to indicate the level of background noise after one day of integration. The detection range for ACCESS is the area above the blue curve at bottom right.

Probe of Zodi Dust as a Potential Problem for Terrestrial Planet Detection: High levels of exozodiacal dust will be a major impediment to direct imaging of extrasolar terrestrial planets, no matter what telescope architecture is eventually employed (Beichman et al. 2006). These dust clouds reflect starlight and emit in the thermal infrared, adding photon noise and scene confusion to exoplanet signals. It is therefore crucial to assess the dust levels around nearby stars. The Keck and LBT interferometers use 10 μm nulling observations to probe HZ dust. However, atmospheric and instrumental phase instability has limited the achievable null depth thus far to sensitivities of roughly a hundred zodis. Additional ways to attack the problem are needed. Detailed coronagraphic imaging simulations show that ACCESS can provide sensitivity down to the sub-zodi level, extending inward to 3 AU across the full target sample envisaged for a Terrestrial Planet Finder (TPF) mission, and in to 1 AU for about a dozen stars. Transport models can be used to relate dust levels at 3 AU to those at 1 AU; for our solar system, these models are well-calibrated by dust counts from interplanetary probes. Reflected light observations with ACCESS will thus be an outstanding tool for assessing the dust content in the HZs of nearby stars.

Zodi Structure as an Indicator of Unseen Planets: ACCESS will make the most sensitive imaging survey to date of tenuous debris disks, the signposts of planetary systems. These are clouds of small dust grains created by the mutual collisions of asteroids and comets, as well as by comet sublimation. Without continual replenishment by such events the dust would be cleared away within a small fraction of a star's lifetime by stellar radiation, stellar wind pressure, or self-radiation. The interplanetary dust cloud in our own solar system, which can be seen as the zodiacal light, is a debris disk created primarily by the collisions of asteroids. Spitzer observations have identified more than

80 stars within 25 pc that possess debris disk analogs to our Kuiper Belt, at the levels of a few hundred zodis. Some of these dust clouds have been spatially resolved and show warps, asymmetries, or narrow rings that are strongly suggestive of planetary perturbations. The structure of the eccentric, sharp-edged Fomalhaut debris ring demanded a nearby planetary perturber which was spectacularly confirmed by recent HST (Kalas et al. 2008). Another example is dust in our own solar system resonantly trapped with the Earth (Dermott et al. 1994). Hundreds of nearby stars are likely to have debris disks that can be imaged with ACCESS contrast capabilities at 1 AU resolution. As a canvas on which planets can impress dynamical signatures, dust disk structures will enable indirect detections of numerous planets too faint or too distant to be discovered any other way.

General Astrophysics with ACCESS

Extending a thousand times beyond the performance of HST, the contrast capabilities of ACCESS will enable groundbreaking studies of circumstellar matter and quasar/AGN host galaxies.

For protostellar amd protoplanetary disks, thousands of targets are known within 500 pc from IRAS and Spitzer surveys but very few have been detected against the glare of their central star. Imaging detections to date have taken place largely in special circumstances of external illumination (Bally et al. 2000), edge-on orientation (Burrows et al. 1996), or large central clearings (Krist et al. 2000). At the contrast levels accessible to HST, JWST, and ground-based AO, numerous disks are unseen, perhaps because of dust grain evolution or settling which can produce self-shadowing in these optically thick systems (Dullemond and Dominik 2004). These dimmer, more evolved disks will be revealed around young stars by ACCESS. The disk structures seen will trace the disk dispersal process (possibly showing radial zones cleared by protoplanets), and measure the dust content as a function of age as the systems evolve toward main sequence debris disks.

For post-main sequence stars, ACCESS will image the shell structures which trace the mass-loss that takes place in the Red Giant and Asymptotic Giant Branch regions of the HR diagram. The effect of low-mass companions and pre-existing debris disks on these outflows is thought to be very important for defining the variety of structures seen in the subsequent planetary nebula phase. These outflows seed the ISM with processed gas and dust leading to the next generation of stars and planetary systems. Furthermore, the large luminosity increases of an Red Giant star (~30-100 Lsun) should lead to evaporation and disintegration of any Kuiper belt that was present during the prior main sequence phase, producing a "reborn" debris disk around first ascent red giants and possibly enabling direct imaging of extrasolar comets (Jura 2005).

The Current Trajectory of Exoplanet Science

Over the next decade, how will the current and building astronomy facilities add to our knowledge, and what kind of major new facility can have the greatest impact?

RV surveys are beginning to find "super-Earth" planets in short-period orbits. Around Sun-like stars, they will probe for Neptune-mass planets orbiting within 1 AU and Jupiter-mass planets orbiting as distant as 7 AU. For the very low mass stars, RV should achieve detections of objects as small as a few Earth masses at orbital distances of a few tenths of an AU (Udry et al. 2007). The orbital element distribution for the major inner planets of nearby stars should be well in hand by the end of the next decade.

Upcoming transit observations will reveal the frequency and radii of inner rocky exoplanets by photometrically monitoring large ensembles of solar-type stars. COROT is apparently finding examples of large terrestrial planets in short orbital periods, while Kepler will probe for Earth-mass planets in 1 AU orbits. Spectroscopic measurements made during transit and secondary eclipse by warm Spitzer, the upgraded HST, and JWST will constrain their albedos and detect high opacity atmospheric species such as Na I, CH_4, and Ly a (Charbonneau et al. 2007). By the middle of this coming decade, transit work should have yielded a statistical understanding of the inner parts of

extrasolar planetary systems.

High contrast imaging detections of self-luminous exoplanet and brown dwarf companions are expected from large ground-based telescopes deploying the next generation of adaptive optics systems, and from space using JWST. Contrasts of 10^{-7} are projected at 0.2 arcsec separation in the near-infrared (Beuzit et al. 2007), extending well beyond today's performance of 10^{-5} contrast at 1 arcsec. This would enable detection of warm (young/massive) gas giant planets with today's 8-m class telescopes, while an optimized 30-m telescope would extend this to a 0.07 arcsec inner working angle. At 4.5 μm, JWST's NIRCam coronagraph will be capable of detections at contrasts of 10^{-6} at separations beyond 1.5 arcsec, capturing objects like our own Jupiter in thermal emission as companions to the nearest M stars (Krist et al. 2007). The uncertain luminosity evolution of young giant planets clouds the picture somewhat (Marley et al. 2007), but it appears that the outer, massive planets orbiting nearby (d< 20 pc), young (age < 1 Gyr), low-mass (M < 0.5 Msun) stars could be in view midway through the coming decade.

Imaging of protoplanetary disks will be revolutionized by ALMA, which will be able to resolve dynamical structures driven by protoplanets at angular resolutions approaching 0.01 arcsec. For the more nearby debris disks, ALMA will be able to map systems brighter than 1000 zodis at 0.1 arcsec resolution. A 5σ detection of the Fomalhaut debris ring surface brightness can be achieved at 450 μm in 6 hours at this resolution, according to the online ALMA sensitivity calculator. At 20 μm JWST will resolve warm debris around nearby A stars with 0.3 arcsec resolution. Large ground telescopes with adaptive optics operating in the near-IR will push toward the 1000 zodi sensitivity benchmark established by HST. Herschel will detect exoKuiper belts down to the ~10 zodi level. A wealth of new data detailing the internal structure of bright circumstellar disks will be emerging in 2015, seeding a new theoretical understanding of disk structure, dynamics, and evolution.

The ACCESS Mission

While the advances described above will be remarkable scientific milestones, these existing and developing facilities fall well short of the objective of obtaining resolved images and spectra of dynamically full exoplanetary systems like our own, systems that may harbor terrestrial planets in habitable zones. Are such systems commonplace? Given that ACCESS could provide the first spectral measurements from a dozen or more RV planets, and a census of yet unknown exoplanets orbiting between 3 and 20 AU from their stars, and quite possibly a number of super-earths, the impact on exoplanet science could be huge. We know essentially nothing about exozodiacal dust disks at the level of our solar system, yet these disks are signposts of planetary systems and unseen planetesimals, and their eccentricities and asymmetries are sensitive indicators of unseen planets. An ACCESS survey of many such systems would provide compelling evidence for the nature and prevalence of exoplanetary systems. ACCESS offers a pathway to the nearby exoplanet systems, by way of giant planets and debris structures, for more than 100 stars within ~20 pc. ACCESS is a compelling and logical next step for NASA's Exoplanet Exploration Program.

ACCESS Technical Overview

Pictured here are three views of the ACCESS observatory. The main observatory elements are the telescope, spacecraft, precision pointing control system, and a high-contrast coronagraph camera. A raytrace diagram of the optical system, including the telescope and coronagraph, is illustrated at right.

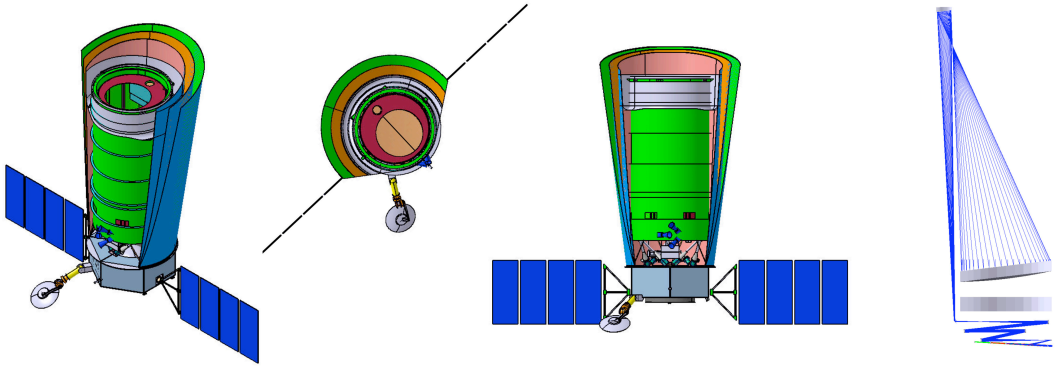

Telescope

The telescope optical design is an unobstructed off-axis Gregorian design that delivers a diffraction-limited visible image to the science instrument coronagraph. At the heart of the optical telescope assembly (OTA), is the system's 1.5 m lightweight (areal density of 40-50kg/m^2) primary mirror. Due to the stringent stability requirements for the system, the glass for the PM and secondary mirror is specified to be the highest quality ULE® glass. The PM is constructed in a manner similar to that for the fabrication of the Advanced Mirror System Demonstrator (AMSD) optic, which was built under funding of a consortium of government agencies including NASA. The PM has front and back facesheets and a light-weighted core formed by abrasive water jet. The three components are fused together, resulting in a mirror that is pure ULE®, enabling the most thermally stable optic possible.

The prescription for the optical figure of the PM was chosen to be identical to the 1.8m Technology Demonstration Mirror (TDM) funded by the TPF program. This decision was made to mitigate risk on the ACCESS mission because the metrology null that was to be used to test the TDM has been manufactured and calibrated. Calibration results showed that the uncertainty in the null was ~2nm-rms, fitting within the wavefront and contrast error budget for ACCESS. ITT has already achieved these wavefront requirements on optics in a similar size class to ACCESS.

The precision structures of the optical telescope assembly design benefit from commonality with TRL9 components of the 1.1m high-resolution NextView Electro-Optical payload developed by ITT, which was launched in September 2008. This maximizes the use of high TRL hardware, materials, and proven design and manufacturing processes.

Spacecraft

The spacecraft bus provides all housekeeping functions for the observatory, including power, propulsion for orbit insertion and maintenance, attitude control, command and data handling, communications, and thermal control of the bus itself. The spacecraft bus also serves as the primary structural interface to the launch vehicle, the sunshade, the Optical Telescope Assembly (OTA) and the Outer Barrel Assembly (OBA). A V-groove sunshade, derived from the JWST design, ensures that changes in observatory orientation will not adversely affect the telescope thermal environment. The spacecraft structure draws from NG's modular Advanced Bus family of products. The bus has an aluminum hexagonal structure with a central cylinder and six shear panels

to support the telescope and instrument. The central cylinder is sized for direct attachment to the Atlas V and carries the primary structural loads.

The propulsion subsystem provides a reaction control capability for the observatory. It is used for trajectory correction maneuvers after launch and during cruise to a Sun-Earth L2 halo orbit, for halo orbit insertion, and for station keeping and momentum dumping. It can also be used for attitude control during contingency operations. The propulsion subsystem is sized for 10-years of operation, with total delta-V budget of 150 m/s. The propulsion subsystem uses a simple, flight-proven hydrazine mono-propellant system, which has a capacity of 225 m/s, providing 33% margin. One 4.45 N thruster is used for delta-V maneuvers and three 4.45 N thrusters are used for attitude control.

Pointing Control System

The precision pointing control system (PCS) for ACCESS has been developed with the objective of defining the best available within the cost constraints of a medium-class space coronagraphic observatory with current high-maturity technology (TRL 6 or above). ACCESS requires a high precision Pointing Control System because pointing errors adversely affect image contrast in two ways: (1) decentering of the star on the focal plane mask to produce light spillage outside the mask, and (2) telescope pointing errors lead to beam-walk of the corrected wavefront over the optics upstream of the fine steering mirror.

The three-stage pointing system starts with a standard 3-axis stabilized spacecraft bus and it is augmented with an ITT AIMS hexapod pointing system to stabilize the telescope line of sight, and a fine steering mirror within the coronagraph. AIMS provides closed loop active dynamic control to isolate the optical payload from reaction wheel disturbances on the spacecraft bus, enabling telescope pointing stability that is several times better than Hubble. The ACCESS design is the result of a close collaborative effort among engineers at JPL, NG, and ITT, who have designed the PCS on the basis of dynamic models of the observatory structures (FEM models for the spacecraft bus, solar arrays, telescope, hexapods, and a lump mass model for the coronagraph); end-to-end optical propagations models for the telescope and coronagraph system, and models for the spacecraft ACS system, the hexapod pointing systems, the fine steering mirror, the fine guidance camera and the control architecture.

Mission description

The mission begins with a launch from the Cape Canaveral Air Force Station aboard a Delta IV or Atlas V-class vehicle. The launch puts the observatory on a direct trajectory to the Sun-Earth Lagrange point 2 (L2), where the system enters into a halo orbit for a prime mission of 5 years. This orbit provides a stable thermal environment and the ability to observe a large fraction of the sky, while requiring a delta-V of only 20 m/s to maintain the orbit for the 5 years.

The total mass of the observatory (telescope, coronagraph, wet spacecraft) is 2074 kilograms, including an overall 20% contingency based on the maturity of the individual components. The smallest variant of the launch vehicle class, the Atlas V-401, provides a lift capacity to L2 of 3793 kg, hence a lift mass margin of 45%. The observatory fits within the Atlas standard, 4-meter diameter, Extended Payload Fairing. The maximum power load of the observatory is 1916 watts, including a 30% contingency for growth. The solar array capability is 2568 watts at end-of-life, providing an additional 25% margin beyond the contingency. The arrays are sized for the 30° off-pointing required during rolls.

The observatory is designed to access stars outside a solar avoidance angle of 80 degrees. To minimize thermal settling time following a slew from one target star to another, ACCESS will normally restrict the angle between the Sun and target star to a range between 80 and 120 degrees. The yearly rotation of the observatory around the Sun then provides natural observing windows for

two or more visits of any target star per year.

The Deep Space Network is used for telecommunications. The radio frequency is S-band. Data volumes of about 3 GB are downlinked twice per week. Observing sequences are uplinked during downlink passes. Estimates are that two passes of 8 hours each per week support nominal operations. Engineering data is routed to a JPL operations center for pipeline analysis, distributed to investigators for further analysis, and finally archived.

Coronagraph Configurations

ACCESS has compared four coronagraphs representative of the major coronagraph types, indicated schematically in the figure below. Here we describe the elements of the ACCESS coronagraph instrument that are common to all four types. Then we describe the unique coronagraph elements that distinguish each of the architectures and define the physical models for our comparisons.

The coronagraph optical assembly is structurally attached to the bulkhead of the optical telescope assembly, which includes the telescope primary and secondary mirrors, a fold mirror, and a collimating mirror. The instrument receives the collimated beam and relays an image of the primary mirror (the pupil of the system) to a 48 mm (2300 actuator) deformable mirror mounted in a gimbaled tip/tilt fine steering mechanism. The optics to this point define the telescope line of sight (LOS), which is stabilized on the sky to 1 milliarcsecond (3σ) with the AIMS attitude control system. The beam passes to a second 48 mm deformable mirror in a fixed mount, then to a paraboloidal mirror that brings the beam to a focus. The image of the target star is stabilized at this focal point to 0.45 milliarcseconds (3σ) using the pointing knowledge from the fine guidance camera. Therefore, all coronagraph instruments share an observatory platform that provides (1) a stabilized telescope LOS, (2) an internal fine guiding sensor and tip/tilt mechanism that stabilizes the star image at the first instrument focus, and (3) a pair of high-TRL precision deformable mirrors for wavefront control. Optical elements specific to each coronagraph type follow this common "front end", and are described below.

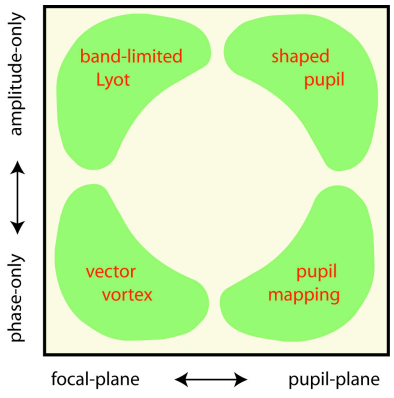

Following the unique coronagraph optics, there are the "back end" elements common to all four coronagraphs. These elements use dichroic mirrors to split the light into three 20% spectral bands (500-600 nm, 600-720 nm, and 720-870 nm), then project these spectrally filtered high-contrast images simultaneously onto a single low-noise CCD focal plane. An integral field spectrograph, with resolving power of 20, receives light from a selected area in the coronagraph dark field by means of a steerable mirror. Finally, a realistic physical description of these optical elements, derived from measured characteristics of commercially available components, are embedded in an optical diffraction propagation model written in IDL using the PROPER library of coronagraph elements (Krist 2007). The elements unique to each coronagraph type are described in the following sections.

Lyot Coronagraph: The band-limited Lyot coronagraph was introduced by Kuchner and Traub (2002) and extended to higher-order apodizations by Kuchner et al. (2005). These band-limited masks have been manufactured most recently as vacuum-deposited metal films on glass. The highest contrast results to date have been obtained with a Lyot coronagraph in JPL's High Contrast Imaging Testbed (HCIT; Trauger et al. 2008). Recent work has shown that hybrid metal-dielectric masks, band-limited in both real and imaginary parts, can achieve high contrast over bandwidths of 20% with useful throughputs of order 65% (Moody et al. 2008). Analysis has shown that a trade can be made between useful throughput and inner working angle, and that IWAs as small as 2 λ/D are feasible. The testbed has also demonstrated open-loop contrast stability of 10^{-11} over periods of five hours or more (Trauger and Traub 2007), enabling post-observation image subtraction techniques

that demonstrate contrasts better than 10^{-10}.

Vector Vortex Coronagraph: The phase mask coronagraph has been developed in a number of forms, including most recently the vector vortex mask (Mawet et al. 2005). Our main interest lies in the performance and readiness of phase vortex masks designed for topological charge of 4 or greater. The new mask is implemented with a liquid crystal polymer technology developed by JDSU. The technology provides a natural pathway to achromatized phase masks capable of a 20% bandwidth at a contrast of 10^{-9}.

Shaped Pupil Coronagraph: The shaped pupil coronagraph was introduced by Spergel (2000) and developed at Princeton (Kasdin et al. 2005). Physical masks have been manufactured from silicon wafers at JPL's Micro Devices Laboratory and validated in tests in JPL's HCIT. The "Ripple 3" design has achieved 2×10^{-9} contrast with a spectral bandwidth of 10% over a field of view spanning 4-10 λ/D. The shaped pupil masks to date have been limited to an inner working angle of 4 λ/D, where a hard-edged focal plane mask blocks the direct light from the star. Inner working angles smaller than 4 λ/D can be achieved only by adding an element of pupil mapping to the coronagraph,as described by Pueyo et al. (2007), who showed that , in principle, the use of a pair of deeply-figured mirrors in conjunction with the shaped pupil could improve coronagraph IWA to 2.5 λ/D. We note that in this approach, the shaped pupil concept takes on some characteristics of the pupil mapping coronagraph.

Pupil Mapping Coronagraph: The pupil-mapping system (Guyon 2006), also known as phase induced amplitude apodization (PIAA), uses a pair of steeply aspheric mirrors to concentrate and apodize the light towards the center of the coronagraph pupil. PIAA can in principle achieve high contrast and high throughput at inner working angles of 2 λ/D. Guyon et al. (2005) and Belikov et al. (2006) have shown that additional grey-scale or binary apodizations are needed to suppress wavelength-dependent diffraction effects, leading to hybrid designs that achieve in principle bandwidths of 20% and throughputs of order 85%. Studies have been made of the pupil-mapping coronagraph with one or two deformable mirrors (Shaklan et al. 2007). The best reported laboratory performance with the first generation of PIAA mirrors is a contrast level of 2.2×10^{-7} averaged between 1.6 and 4.4 λ/D in monochromatic light (Guyon 2009). Manufacturing of the PIAA mirrors is challenging. A second generation of PIAA mirrors has been fabricated by Tinsley and will begin laboratory testing in the HCIT in spring 2009.

Coronagraph Implementation

An optical schematic and mechanical concept for a Lyot version of the coronagraph appear below. The vector vortex and shaped pupil options are similar, using different coronagraph masks inserted into the same layout of mirrors and mechanisms. The pupil mapping option is taller, requiring six additional mirrors in the optical path and two additional mechanisms. All options feature redundant assemblies of these critical elements for single-point fault tolerance: fine guidance cameras, deformable mirrors, and science cameras. These bands are focused simultaneously onto adjacent areas of a single CCD detector or to the spectrograph.

The mechanical concept uses low CTE materials for dimensional stability. Stack height (vertical in the figure) is a critical dimension so as not to outgrow the launch vehicle fairing. The Lyot, vector vortex, and shaped pupil options fit with 0.4 m of stack height to spare. The pupil mapping option fits but with little margin. Cameras are placed out of plane for easy access during integration and test and to simplify temperature control of the detectors. Access panels (not shown) exist so that other elements are readily accessed for troubleshooting and alignment without forcing major disassembly of the instrument. All options feature several, single-fault tolerant mechanisms. Where possible, the same mechanism design (e.g., a linear positioner) is repeated. Temperature stability is achieved by using blankets, electrical heaters, and heat pipes.

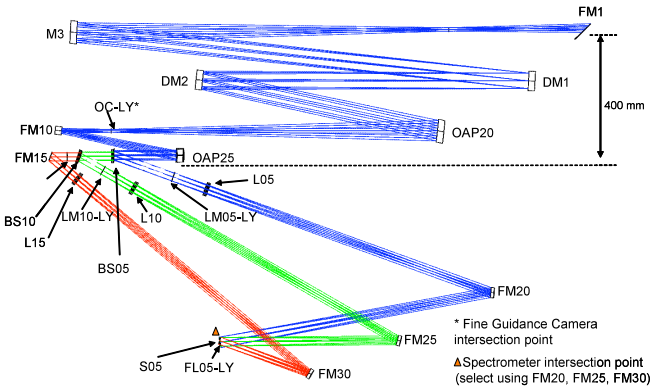

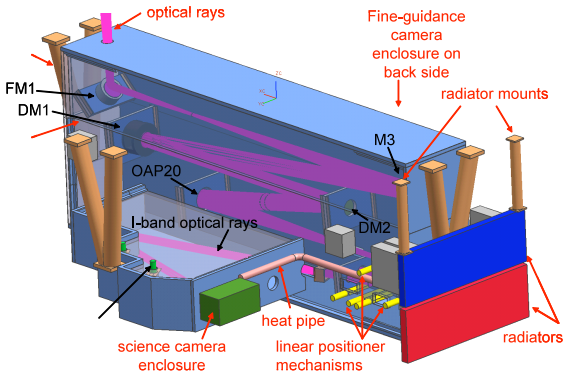

ACCESS coronagraph performance floor

We define a coronagraph performance floor based on coronagraph technology already demonstrated in the laboratory as of March 2009. This point in performance trade space can be used to define a minimum science reference mission for the ACCESS mission.

Here we collect the demonstrated laboratory results as of March 2009, and plot them in the adjacent figure, as follows. (a) Lyot coronagraph contrasts with an inner working angle of 3 λ/D are results obtained with a hybrid mask (Moody et al. 2009) on the HCIT in March 2009. The plotted contrast values are intensities measured in the floor of the high-contrast dark field normalized to the intensity of the central star, averaged separately over an "inner" region (3-4 λ/D) and an "outer" region (3-10 λ/D). The measured contrasts were equal in the inner and outer regions, for both 10% and 20% bandwidths. Historically, Lyot coronagraph contrasts for the IWA of 4 λ/D are taken from TPF-C Milestone #1 Report (Trauger, Kern, Kuhnert 2007) for monochromatic light and from TPF-C Milestone #2 Report (Kern, Kuhnert, Trauger 2008) for 10% bandwidth, and again refer to the average contrasts measured in both the "inner" region (4-5 λ/D) and the "outer" region (4-10 λ/D) of the high contrast field. Wavefront sensing and control for all Lyot contrast measurements were carried out over a half-dark-field with a single Xinetics 32×32-actuator deformable mirror using either the speckle nulling or EFC algorithms and images in the coronagraph focal plane. (b) Vector vortex results obtained in February 2009 on the HCIT with the first manufactured example of a phase mask based on the liquid crystal polymer technology from JDSU (Mawet et al 2009). The mask was measured to have an IWA of 1.8 λ/D, in close agreement with the vortex model. For a 2% bandwidth, the plotted values are again the average intensity measured in the high-contrast dark field normalized to the intensity of the central star, averaged over an "inner" region (3-4 λ/D) and an "outer" region (3-10 λ/D). Wavefront sensing and control was carried out over a half-dark-field with a single Xinetics 32×32 deformable mirror and EFC using images in the coronagraph focal plane. (c) Pupil mapping result obtained in the ambient air at the Subaru coronagraph laboratory (Guyon et al. 2009). The plotted contrast value is the contrast averaged over a half-dark-field extending from 1.6 to 4.4 λ/D, obtained in monochromatic 633 nm laser light with a single Boston Micromachines 32×32 deformable mirror, using a variation on the EFC algorithm for wavefront sensing and control. (d)

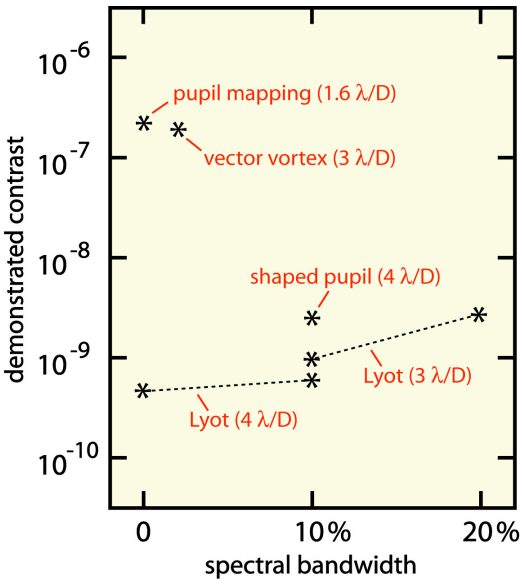

Shaped pupil results are from experiments performed on the HCIT (Belikov et al 2007). Wavefront sensing and control was carried out over a half-dark-field with a single Xinetics 32×32-actuator deformable mirror using speckle nulling at the central wavelength of the 10% spectral band.

From among these, we select the Lyot coronagraph demonstration of 10^{-9} contrast with inner working angle of 3 λ/D and a spectral bandpass of 10% centered on 550 nm as representative of the currently-demonstrated state-of-the-art and the performance floor for ACCESS.

ACCESS science capability floor

We have carried out a model run for a conceptual space coronagraph with the characteristics of this specific Lyot coronagraph, leading to images of the high contrast coronagraph field and the corresponding minimum science program.

The elements of a model run are as follows. (1) All modeling presumes the baseline ITT telescope, NG spacecraft, ITT/AIMS stabilization of the telescope line-of-sight, fine pointing control with the Xinetics fine steering mirror internal to the coronagraph, precision wavefront control with a pair of Xinetics 48×48 actuator DMs, JPL/ITT observatory thermal control system, and the instrument optical layouts that have already been defined by the ACCESS engineering team; (2) end-to-end (i.e., including all optical elements from star to coronagraph focal plane) Fresnel propagation implemented in PROPER code or equivalent; (3) surface figure errors assigned to each optical element, consistent with the state-of-the-art surface PSDs for commercial optics; (4) our standard model for Xinetics deformable mirror surface influence functions, with DM settings for a high-contrast dark field derived using EFC nulling algorithms (Giveon et al. 2007); (5) Monte Carlo simulations of pointing control dynamics, based on ACCESS analysis of telescope LOS pointing jitter (1 mas 3σ) and knowledge-limited pointing correction accuracy with the fine steering mirror (0.45 mas 3σ for a V=7 star); (6) simulation of the dominant effects (drift in primary mirror surface figure and mutual misalignment of the primary and secondary mirrors) of the thermal response to a 30° roll of the observatory about the line of sight to the star (with γ = 100°); where (7) inner working angle is stated in terms of λ/D on the sky, lambda is the central wavelength of the spectral band (e.g., λ = 550 nm for the 10% [525-575 nm] band) and D is the full diameter of the telescope primary mirror; then (8) a set of monochromatic PSFs is computed at wavelengths spaced evenly across the 10% spectral band, using the known wavelength-dependent effects of the coronagraph elements, then averaged together with appropriate weighting to represent the PSF over the full spectral band; leading to (9) the product, a coronagraph high contrast PSF sampled at 5 pixels per λ/D on the sky.

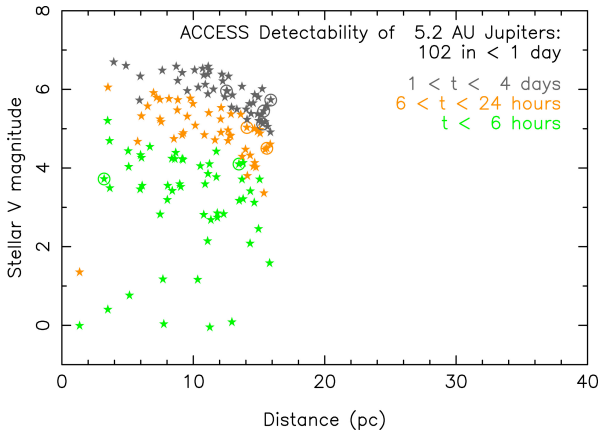

These simulated ACCESS images are then used to predict sensitivities for exoplanet imaging among the nearby stars. For example, the diagram shows the integration time required for 10σ detections of a standard cool (5 Gyr) planet of jovian mass in reflected starlight orbiting the AFGK stars within 16 pc. The planet is assigned an orbital position 45 degress from elongation. Circled symbols indicate those stars already known to harbor major planets based on RV surveys. The exercise illustrates that 102 stars within 16 pc could each be imaged with 10σ sensitivity for a Jupiter twin in integration times of 24 hours or less. As indicated in the previous section, this capability leads directly to a capable program of exploration of the nearby exoplanetary systems. Further advances in the coronagraph technology are expected in the coming year, leading to a still more capable mission.

ACCESS Technology Drivers

Coronagraph performance demonstrations expected by the end of this year: Ongoing laboratory work is likely to advance the demonstrated state-of-the-art coronagraph in a number of predictable ways during the coming year, in advance of a possible NASA AO for a medium-class exoplanet mission. Here we describe technology developments that are currently in progress along specific well-defined technology pathways. In most cases, it is possible to accurately model the expected outcome of these developments and predict the corresponding performance of the coronagraph.

Models of the Lyot coronagraph laboratory performance have been consistently able to predict the sensitivities of coronagraph contrast to measured characteristics of the coronagraph masks with ~10-20% accuracy. These models provide specific guidance for the ongoing development of coronagraph mask technology. The Lyot coronagraph work scheduled for the remainder of this year is as follows. Further design adjustments will be carried out to improve the contrast of the hybrid Lyot mask from 2.6×10^{-9} to better than 1×10^{-9} across a 20% spectral bandwidth. A hybrid (metal and dielectric) focal plane mask with a 2.5 λ/D inner working angle will be fabricated and tested on the HCIT. Lyot experiments on the HCIT will also include, for the first time, wavefront control with two deformable mirrors in sequence, thus testing our models for the creation of 360 degree "two-sided" dark fields with improved contrast and bandwidth.

A second-generation vortex mask has been ordered from JDSU and will be tested on the HCIT during the remainder of this year. This mask will implement refinements in the fabrication process to reduce internal reflections and reduce the dimensions of the central vortex singularity. The vortex coronagraph model, guided by recent HCIT experience with the first-generation mask, predicts that these refinements will provide an improvement by two orders of magnitude over the currently demonstrated contrast of 2×10^{-7} in narrowband (2%) light. In addition, the design will be extended to achromatize the vector vortex mask, with the model prediction of 10^{-9} contrast over a 20% spectral bandwidth.

HCIT experiments have been initiated with second-generation pupil mapping coronagraph elements. A pair of pupil mapping mirrors, commissioned by NASA/Ames and fabricated by Tinsley according to a second-generation PIAA design by Guyon, are now resident on the HCIT optical table and ready for the first laboratory tests of a pupil mapping system in a vacuum environment. Initial experiments are aimed at high contrast with an expected inner working angle of 2.3 λ/D. Testing will proceed in stages from narrowband laser light to broader bandwidths. Apodizer designs will be tested and refined. Expectations are that the demonstrated contrast will be significantly improved over the current best results, 2.2×10^{-7}, obtained in the ambient laboratory environment at Subaru laboratories.

Coronagraph performance expected in the next 3-5 years: The objective of the ACCESS study is to identify one or more space coronagraph architectures that are already at a high level of technology readiness and ready for a mission proposal in the coming year. The study also identifies the main enabling technologies and critical areas that could be productively advanced in the coming 3-5 years by new investments in known technologies.

First, we point out that the major observatory components are at high TRL. The spacecraft systems are TRL 6 and above. The telescope components are also above TRL 6, save the demonstrated fabrication of a 1.5 meter off-axis primary mirror, which is very similar to high-TRL on-axis mirrors, and which is judged at TRL 5+. The active jitter control for the pointing control system, coupling the telescope and spacecraft structures, is based on TRL>6 systems. Our study has identified the following critical technology drivers.

Deformable mirrors: ACCESS baselines a pair of Xinetics DMs, each consisting of a 48×48

array of electroceramic actuators driving a monolithic fused silica mirror facesheet. These DMs are specifically designed for the precision correction of a diffraction-limited space telescope, and have been developed in a JPL/Xinetics collaboration stretching back to the initiation of a Small Business Innovative Research program ten years ago. These DMs, based on a monolithic PMN ceramic module delineated to form a square array of electrostrictive actuators on a 1 mm pitch, have proven robust, without failure in the actuator structures, in more than 5 years of active use in the HCIT, a space-like vacuum test environment. Manufacturing processes that the mirror is robust to temperatures up to 80 degrees C. Vibration tests to flight qualification levels have been performed successfully on a prototype 48×48 DM, configured for flight including flight-quality electrical connectors and identical in form to the ACCESS DM. We judge the DM technology to be at or near TRL 6.

Low-read-noise CCDs: ACCESS has baselined commercially available CCDs of the type available from e2V for the coronagraph focal plane and the guider camera sensors. These CCDs, AR-coated and backside illuminated for high DQE, with read noise of 3-5 electrons/pixel, have proven robust for space applications, including the soon-to-be-launched WFC3 for the Hubble telescope. These are a low-risk technology.

However, the needs of the spectrograph lead to a still lower read noise requirement. In the spectrograph, with the dispersed light from faint objects diluted 20-fold over the spectrograph pixels compared to the direct coronagraph images, the CCD needs to operate essentially as a photon-counting imager. The LLL avalanche technology from e2V is available and under study for space applications, but has yet to prove its potential for noise-free photon detection. We recommend that the "skipper" technology be advanced in the coming years, to provide a more sensitive integral field spectrograph for exoplanet (and other general astrophysics) missions.

Pupil mapping technology: We recommend investments in three areas critical to the pupil mapping approach. First, an investment in fine-scale (~0.1 mm) ion beam figuring (IBF) of the pupil mapping mirrors, specifically to attack the severe surface requirements for the outer few mm in radius of the M1 (apodizing) mirror. Without an improvement in aspheric figuring methods over that which has been demonstrated to date, pupil mapping performance will suffer from imperfect pupil apodization, leading to requirements for a more aggressive transmissive post-apodizer, reduced overall throughput and degraded inner working angles. Second, we recommend investments to advance the computational techniques for pupil mapping. At this time, the single practical optical propagation algorithm with the fidelity required for end-to-end modeling of the pupil mapping coronagraph is the S-Huygens method (Belikov et al. 2006), which is too slow for the many passes needed for setup of the wavefront control matrices and for optical tolerancing of the actively-corrected space coronagraph system. For example, the S-Huygens propagation from pupil mapping M1 to M2 involves the propagation of at least 400 azimuthal harmonics. The computation time for one end-to-end pass through the ACCESS optical system, which includes both a forward and reverse pair of pupil mapping mirrors, takes about 2.5 hours using an 8-processor, 64-bit, 3 GHz computer. Third, a trade analysis of the optimal layout of pupil mapping and deformable mirrors. The ACCESS layout, for example, with DMs placed prior to the pupil mapping mirrors, provides a relatively large field of view, but also leads to a requirement for extremely high quality (~0.25 nm rms EUV lithography grade surfaces) in the optics between the pupil mapping mirrors and the occulting mask in order to achieve contrast better than 10^{-9} in a 20% bandwidth. These technology issues have generally been addressed by Belikov et al. (2009).

Vector vortex technology: The vortex mask reported in this study is the first of its kind, and the result of only a small initial technology investment. The JDSU liquid crystal polymer technology is a pathway to a future high-contrast vortex mask that could be achromatic over 20% spectral bandwidths. The vortex coronagraph is as simple to implement as the Lyot coronagraph, and promises higher overall throughput, and is therefore worthy of strategic investment.

Activity Organization, Partnerships, and Current Status

The ACCESS study draws upon the partnership of an experienced team from JPL, Northrop Grumman Aerospace Systems, ITT Space Systems Division LLC, and NG-Xinetics. Development of the ACCESS concept benefits from our collaborations (over the past ten years) on the closely related Eclipse proposal to NASA's Discovery program in past years, hence many of the basic engineering trades, system engineering models, and general knowledge of the unique challenges of this concept have been studied and widely communicated across the entire science and engineering team. This activity is focused on the design of a medium-class NASA mission, for which cost credibility is of central importance. Our approach is to clearly define the science mission, then develop a mission design that builds upon the special expertise and well-understood methods and technologies resident at JPL and its industry partners, thereby to base our estimates of cost and schedule on a reliable foundation of experience. Further, the ACCESS partners are prepared to utilize an integrated Earned Value System to manage cost, risk, and schedule during development. The ACCESS team believes that the concept is "proposal ready" for a mission in the coming decade.

Activity Schedule

The figure below shows the proposed schedule for the project. The proposal and selection process for a medium-class mission is presumed to take about 16 months and serves as phase A of the project. The duration of phases B/C/D is 51 months with a one-month launch period. The 51-month duration is shown, which includes 2 months of margin on the critical path during integration and test. The amount of margin is consistent with the JPL flight project guidelines. These milestones are separated by typical durations, for example, the Project CDR is scheduled about 11 months after the Project PDR.

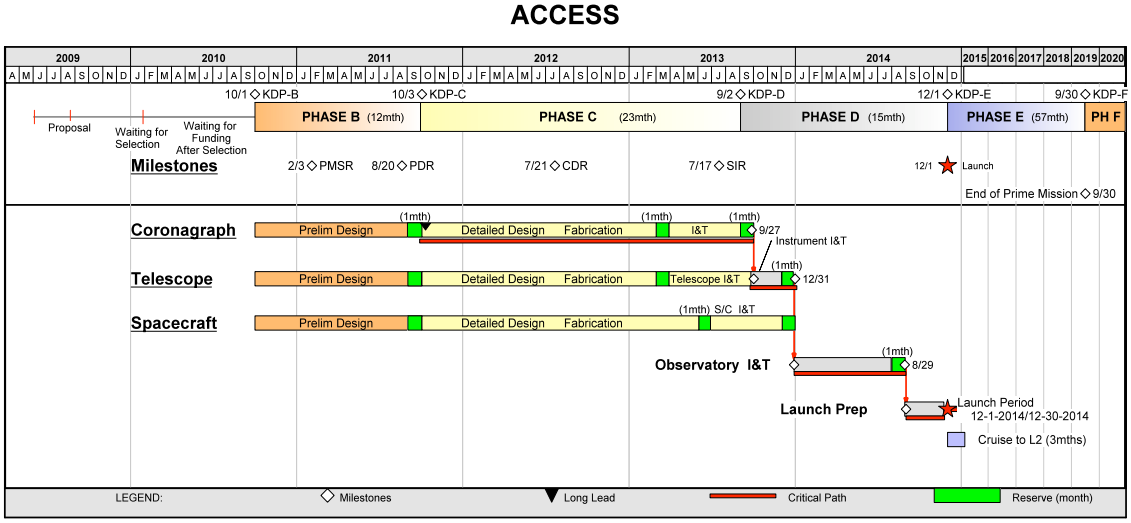

Assembly, integration, and test (AI&T) activities include coronagraph, telescope, and spacecraft mechanical build-up and integration, electrical integration, software integration, comprehensive performance test, observatory mechanical and electrical integration, observatory environmental tests, and observatory launch preparation. Existing facilities at JPL and its industry partners are sufficient for the test campaign. The three main AI&T activities are performed in parallel: coronagraph I&T at JPL, telescope I&T at ITT, and spacecraft bus I&T at NG and its

subcontractors. These components are then electrically and mechanically integrated and unit performance tests are conducted.

After calibration at JPL, the coronagraph is shipped to ITT's Rochester, NY facility for mechanical and electrical integration with the telescope and an end-to-end optical performance test of the assembled instrument. At the same time, the spacecraft bus is mechanically and electrically integrated at NG's Redondo Beach, CA facility and undergoes comprehensive performance testing to demonstrate satisfactory operation of the spacecraft hardware and software. Following a successful Payload Integration Readiness Review, the instrument (telescope and coronagraph) is shipped to NG. With support from JPL and ITT, NG integrates the spacecraft bus and the instrument; tests the performance of the observatory for shipment; and transports it to the launch site for integration.

Several end-to-end systems tests are performed during I&T and launch site operations. This includes RF compatibility tests of the RF links to verify all telemetry and command control functions, and simulated mission operations of the observatory by the mission operations team and ground system during comprehensive performance and thermal vacuum tests. The comprehensive performance tests include end-to-end test of the attitude control subsystem and science camera with an instrument stimulus (a sub-aperture collimated light source) to check the instrument error signal control loop and overall instrument performance.

Cost Estimates

Necessary technologies are to be matured to at least TRL 6 by the end of Phase B. ACCESS benefits from the substantial technology development investments already made for the Terrestrial Planet Finder mission. Technologies requiring additional maturation are limited primarily to component technologies within the instrument; therefore, the risk to cost and schedule associated with technology development is considered to be modest.

The ACCESS concept was submitted for detailed review by JPL's Team X concurrent engineering team for mission formulation studies, so that an independent cost estimate could be produced consistent with other current astrophysics mission concepts.

Team X guidelines for the ACCESS study were to provide independent design and costing analysis for the mission concept. Project-provided designs were used, but not project-provided cost estimates. The cost estimates summarized in this document were generated as part of a Pre-Phase-A preliminary concept study, are model-based, were prepared without consideration of potential industry participation, and do not constitute an implementation-cost commitment on the part of JPL or Caltech. The accuracy of the cost estimate is commensurate with the level of understanding of the mission concept, typically Pre-Phase A, and should be viewed as indicative rather than predictive. Following Team-X guidelines, the cost estimate includes 30% reserves for development (Phases A-D) and 15% for operations (Phase E). This cost estimate, summarized in the table, was provided by Team-X in March 2009.

Mission cost is roughly $830M FY09 with appropriate contingencies, including 5 years of science operations. Details are shown in the table that follows. We note that this Team-X cost estimate is consistent with an overall cost estimate developed independently by the ACCESS engineering team, including JPL and industry partners, based on a detailed bottom-up cost estimate for components, subsystem and system integrations and tests, and mission operations.

While fundamentally a different instrument and capability, the Kepler mission provides a reality check for ACCESS costs. Kepler carries a single instrument and a space telescope with a 1.4 m diameter primary mirror in a drift-away orbit. ACCESS is a 1.5 meter space telescope with a single instrument in an L2 orbit. The duration of Kepler's prime mission is 3.5 years, while ACCESS's is 5 years. Both observatories are solar powered. Both missions seek to observe exoplanets. Both missions are partnerships between JPL and experienced aerospace systems companies. A major

difference is that Kepler's attitude stability requirements are not as strict as those for ACCESS. Kepler's requirement is 9 mas (3σ) over 15 minutes whereas ACCESS's is 0.5 mas (3σ), a difference that can be quantified in terms of an attitude control system based on high TRL 6+ components. NASA's February, 2009 Press Kit for the Kepler launch includes this statement: "The project's life-cycle cost is approximately $600 million. This includes funding for 3.5 years of operations." While the quoted cost is in real year dollars rather than FY09 dollars, this suggests that the ACCESS estimate is of the right magnitude and reasonable.

Item	Cost ($M 2009)*
Management, Systems Engr., Mission Assurance	46
Payload System	220
-- Coronagraph (Lyot, Vector Vortex, or Shaped Pupil)	70
-- Telescope	150
Flight System	165
Mission Ops/Ground Data System	60
Launch vehicle (Atlas V-401)	140
Assembly, Test, Launch Operations	16
Science	21
Education and Public Outreach	5
Mission Design	7
Reserves	150
Total Project Cost	830

* Individual WBS elements have been rounded to 2 significant digits.

Phase A	6
Phase B	56
Phase C/D	710
Phase E/F	58
Total	830

Acknowledgements

This research was supported by the NASA Astrophysics Strategic Mission Concept Studies initiative. The work was performed at the Jet Propulsion Laboratory, under a contract with the National Aeronautics and Space Administration.

References

Bally, J., C.R. O'Dell, M.J. McCaughrean 2000. "Disks, Microjets, Windblown Bubbles, and Outflows in the Orion Nebula," A. J., 119, 2919.

Beichman, C. et al. 2006, "New Debris Disks around Nearby Main-Sequence Stars: Impact on the Direct Detection of Planets", Ap.J. 652 1674

Beuzit, J.-L. et al. 2007, "Direct Detection of Exoplanets", in Protostars and Planets V, Univ. of Arizona Press, pp. 717-732.

Belikov, R., et al. 2006. "Toward 10^{-10} contrast for terrestrial exoplanet detection: demonstration of wavefront correction in a shaped pupil coronagraph," Proc. SPIE, 6265, 626518.

Belikov, R., N.J. Kasdin, R.J. Vanderbei 2006. "Diffraction-based Sensitivity Analysis of Apodized Pupil-mapping Systems," Ap.J., 652, 833.

Belikov, R., et al. 2007. "Demonstration of high contrast in 10% broadband light with the shaped pupil coronagraph," Proc. SPIE, 6693, 66930Y.

Belikov, R. 2009, "Overview of Technology Development for the Phase-Induced Amplitude Apodization (PIAA) Coronagraph", Astro2010 technology white paper.

Brown, R.A. 2009, "Science-Operational Metrics and Issues for the 'Are We Alone' Movement", Astro2010 science white paper.

Brown, R.A. 2009, "On the Completeness of Reflex Astrometry on Extrasolar Planets near the Sensitivity Limit", arXiv:0901.4897

Burrows, C., et al. 1996. "Hubble Space Telescope Observations of the Disk and Jet of HH 30," Ap.J., 473, 437.

Charbonneau, D. et al. 2007, "When Exoplanets Transit their Host Stars", in Protostars and Planets V, Univ. of Arizona Press, pp. 701-716.

Dermott, S. et al. 1994, "A Circumsolar Ring of Asteroidal Dust in Resonant Lock with the Earth", Nature 369 719

Dullemond, C., C. Dominik 2004. "Flaring vs. self-shadowed disks: The SEDs of Herbig Ae/Be stars," Astronomy and Astrophysics, 417, 159.

Jura, M. 2005, "Direct Detection of Extrasolar Comets is Possible", A.J. 130 1261

Give'on, A., et al. 2007. "Broadband wavefront correction algorithm," Proc. SPIE, 6691.

Guyon, O., et al. 2005. "Exoplanet imaging with a Phase-Induced Amplitude Apodization coronagraph. I. Principle," Ap. J., 622, 744.

Guyon, O., et al., 2006. "Theoretical limits on extrasolar terrestrial planet detection with coronagraphs," Ap.J.Suppl., 167, 81.

Kalas, P. et al. 2008, "Optical Images of an Exosolar Planet 25 Light-Years from Earth", Science 322 1345

Kasdin, N.J., R.J. Vanderbei, M.G. Littman, D.N. Spergel 2005. "Optimal one-dimensional apodizations and shaped pupils for planet finding coronagraphy," Applied Optics, 44, 1117.

Krist, J. et al. 2000, "WFPC2 images of a face-on disk surrounding TW hydrae", Ap.J. 538, 793.

Krist, J. et al. 2007, "Hunting Planets and Observing Disks with the JWST NIRCam Coronagraph", SPIE 6693, 66930H.

Krist, J.E. 2007. "PROPER: An Optical Propagation Library for IDL," Proc. SPIE, 6675, 66750P.

Kuchner, M.J., and W.A. Traub 2002. "A Coronagraph with a Band-limited Mask for Finding Terrestrial Planets," Ap.J., 570, 900.

Kuchner, M. J., J. Crepp, J. Ge 2005. "Eighth-order image masks for terrestrial planet finding," Ap.J. 628, 466.

Marley, M. et al. 2007, "On the Luminosity of Young Jupiters", Ap.J. 655 541

Marois, C. et al. 2008, "Direct Imaging of Multiple Planets Orbiting the Star HR 8799", Science 322 1348

Mawet, D., P. Riaud, O. Absil, J. Surdej 2005. "Annular Groove Phase Mask Coronagraph," Ap.J., 633, 1191.

Moody, D., B. Gordon, and J. Trauger 2008. "Design and demonstration of hybrid Lyot coronagraph masks for improved spectral bandwidth and throughput," Proc. SPIE, 7010, 70103P.

Pont, F. et al. Eds. 2009, "Transiting Planets: Proceedings of IAU Symposium 253", Cambridge Univ. Press

Pueyo, L., R. Belikov, J. Kasdin, R. Vanderbei 2007. "Performance study of integrated coronagraph-adaptive optics designs," Proc. SPIE, 6693, 669307.

Spergel, D.N. 2000. "A new pupil for detecting extra-solar planets," astro-ph/0101142.

Trauger, J.T., and W.A. Traub 2007. "A laboratory demonstration of the capability to image an Earth-like extrasolar planet," Nature, 446, 771.

Trauger, J., et al. 2007. "Laboratory demonstrations of high-contrast imaging for space coronagraphy," Proc. SPIE, 6693, 66930X.

Trilling, D. et al. 2008, "Debris Disks around Sun-like Stars", Ap.J. 674 1086

Udry, S. et al. 2007, "A Decade of Radial Velocity Discoveries in the Exoplanet Domain", in *Protostars and Planets V*, Univ. of Arizona Press, pp. 685-700.